IEEE Access
Multidisciplinary ⋮ Rapid Review ⋮ Open Access Journal

Received July 3, 2021, accepted July 27, 2021, date of publication August 3, 2021, date of current version August 10, 2021.

Digital Object Identifier 10.1109/ACCESS.2021.3102050

Evaluation of Fuzzy Membership Function Effects for Maximum Power Point Tracking Technique of Photovoltaic System

TOLE SUTIKNO[1,2], (Member, IEEE), ARSYAD CAHYA SUBRATA[2], AND AHMAD ELKHATEB[3], (Senior Member, IEEE)

[1]Department of Electrical Engineering, Faculty of Industrial Technology, Universitas Ahmad Dahlan, Yogyakarta 55191, Indonesia
[2]Embedded Systems and Power Electronics Research Group, Yogyakarta 55191, Indonesia
[3]School of Electronics Engineering and Computer Science, Queen's University, Belfast BT9 5AH, U.K.

Corresponding author: Tole Sutikno (tole@ee.uad.ac.id)

This work was supported by the Ministry of Education, Culture, Research, and Technology (formerly Ministry of Research and Technology/National Agency for Research and Innovation), Indonesia, through a World Class Research (WCR) Scheme under Contract WCR-001/SKPP.ATJ/LPPM UAD/VI2020.

ABSTRACT The photovoltaic generation system (PGS) is considered a potential renewable energy harvesting system. However, the low conversion efficiency of PGS and maximum power point tracking (MPPT) technique are the main challenges that must be solved. In addition, the switching frequency of the converters employed also affects the MPPT system performance. A high gain voltage DC-DC converter is proposed to replace conventional power converter and fuzzy logic controller (FLC) is applied in the MPPT for optimizing solar energy harvesting system. Nevertheless, evaluation of suitable fuzzy membership function is needed for optimal MPPT technique of photovoltaic system. In this paper, FLC of MPPT for photovoltaic application system was built using various membership functions in MATLAB/Simulink environment. The switching frequency of the high gain voltage DC-DC converter is varied to test the robustness of the performance of each FLC membership function. The results showed that the FLC-based MPPT technique for high gain voltage DC-DC converter with GBell membership function type has the capability to track the maximum power point (MPP) accurately and to achieve optimum power conversion. Furthermore, GBell membership showed having stable and consistent performance at various switching frequencies.

INDEX TERMS Maximum power point tracking, fuzzy logic controller, membership function, high gain voltage DC-DC converter.

I. INTRODUCTION

The demand for photovoltaic generation systems (PGSs) shows a graph of significant improvement. The need to meet global issues to reduce the harmful effects of conventional power plants has led to an increase in the demand for PGSs. As it is well known, traditional power plants, which usually use coal as fuel, have negative effects such as the greenhouse effect, pollution, and solid and liquid waste. The development of necessary material processing technology for making photovoltaic (PV) itself has made it increasingly produced and easily available.

However, PGSs that work by harvesting solar energy have a low power conversion. This is because the performance of PV depends on ambient weather conditions such as irradiation and changing temperature [1]–[3]. Under these varying weather conditions, the maximum power point (MPP) received by PV also varies. This is what causes the low PV power conversion efficiency. The maximum power of PV must be extracted to ensure high power conversion efficiency [4]–[6]. The way to increase the power conversion efficiency of PV is by considering the best converter topology possible. Another way is by optimizing the techniques that have been developed by many researchers to track MPP which is commonly known as maximum power point tracking (MPPT) [7]–[45]. Apart from increasing the power conversion efficiency, the MPPT technique can also increase the lifetime of the PV module [8].

There are various MPPT methods. Conventional methods are unstable due to dynamic response and steady-state, thus

The associate editor coordinating the review of this manuscript and approving it for publication was Giovanni Pau.

causing oscillations around the MPP. Another method that is often used because of its reliability is the fuzzy logic controller (FLC) [22]–[27]. The FLC method is suitable to be applied to PV MPPT because it can handle non-linear systems produced by the PV itself due to changing weather conditions [28]. In addition, FLC is also popular because it does not require knowledge of the PV system model [29]–[31].

However, FLC has some disadvantages. One of the shortcomings of FLC is the problem of efficiency which depends on the performance of the system design [16], [41]–[43]. The inherent weakness of FLC is more towards the design of the algorithm development itself, *i.e.* subset, membership function, and rules. Therefore, the development of the FLC algorithm needs to be optimized from the basics in order to provide optimal results. This basic optimization is conducted by choosing the form of membership function that best suits needs. In this research, FLC was employed to assist the high-gain voltage DC-DC converter topology. The test is conducted by varying the irradiation and switching frequency of the converter. Furthermore, various membership functions are discussed and evaluated to find the most suitable type. The final result of this study aims to improve the MPPT technique using FLC with basic optimization by adjusting the membership function according to the topology and switching frequency of the converter used. Designing a membership function is important in an FLC-based control system. Each type of membership function will produce different performance results. Therefore, choosing the most suitable membership function for the system being built is an important thing to consider.

II. HIGH GAIN DC-DC CONVERTER

The converter used in this study was previously initiated by Dahono [46]. It is based on a modified DC-DC buck-boost converter modifications made to produce a converter that has a high gain voltage. Figure 1 shows the high gain voltage DC-DC converter. The resulting voltage ratio is

$$\frac{V_o}{E_d} = \frac{1}{1-\alpha} \tag{1}$$

where α is a transistor Q duty factor.

This converter switching device can be operated to reduce the ripple content of the switching device in a two-phase converter. The RMS value of voltage ripple and the output voltage ripple for the duty cycle of more than half of this converter are shown in (2) and (3), respectively.

$$\tilde{V}_o = \frac{\bar{i}_o}{Cf_s} \frac{\alpha\,(1-2\alpha)}{2\sqrt{3}\,(1-\alpha)} \tag{2}$$

$$\tilde{V}_o = \frac{\bar{i}_o}{Cf_s} \frac{(2\alpha-1)}{2\sqrt{3}} \tag{3}$$

where f_s is minimum switching of the converter.

III. MAXIMUM POWER POINT TRACKING

There are numerous methods used in the MPPT which have their advantages and disadvantages. However, a capable method of optimally tracking MPP is preferred because it ensures maximum power extraction, reliability and efficiency [20], [21]. Conventional methods such as Perturb and Observe (P&O), Incremental Conductance (IncCond), and Hill Climbing (HC) are widely used even to commercial products because of their simplicity. Nevertheless, these methods are unstable due to dynamic response and steady-state, thus causing oscillations around the MPP.

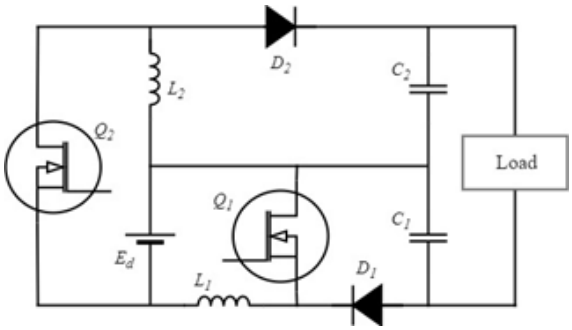

FIGURE 1. High gain voltage DC-DC converter.

Various studies on MPPT based on the FLC method have been carried out and compared with other algorithms, as well as tested through varying the irradiation. These algorithms are built to regulate the duty cycle of the DC-DC converter. Using a boost converter, FLC has better tracking speed and drift avoidance than the P&O, IncCond, and HC methods on dynamic response and steady state (no oscillations) [32]–[34]. Other study conducted by Bendib *et al.* [31] that implemented FLC with a buck converter yielded a similar result. Khateb *et al.* [35] used a SEPIC type converter which was tested with simulation and experimental works. The result obtained is that FLC produces better tracking speed than P&O in both tests. Even the combination of converters, such as buck-boost [36] and boost-SEPIC [37], [38] shows that FLC performance is also superior. Other researches were conducted to find the most reliable but easy to develop FLC performance based on algorithmic design. Hajighorbani *et al.* [39] evaluated a subset of FLC applied to PV MPPT shown that FLC with many subsets produces better efficiency. However, the more subsets that are used, the more the computational burden will be due to the increasing number of rule-bases. Ali *et al.* [40] compared the effect of the FLC membership function but this study was not determined for the PV MPPT purpose.

IV. FUZZY LOGIC CONTROLLER

FLC is based on a statement in the form of a set that is differentiated from other sets based on the degree of membership. In set theory, objects are members, which are denoted by "1", and not members, "0", of a set with crisp membership limits. In the fuzzy set theory, the member of the degree of an object in the set is possible to express the gradual transition of membership in the interval between "0" and "1". The fuzzy set, F, in X is expressed as an ordered pair of the element x.

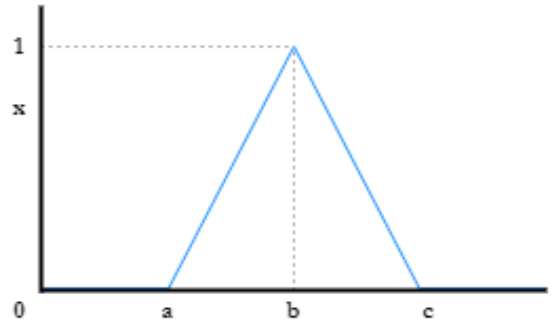

FIGURE 2. Triangular membership function.

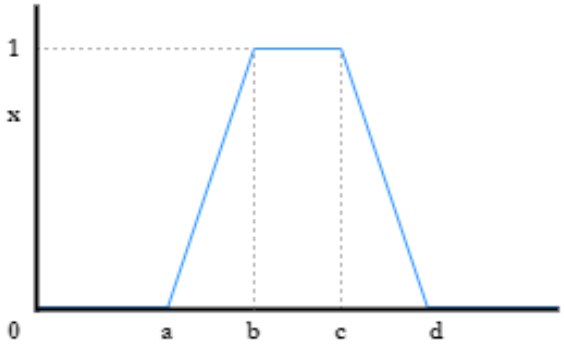

FIGURE 3. Trapezoidal membership function.

The fuzzy set has the membership degrees as

$$F = \{(x, \mu_F(x)) \mid x \in X\} \tag{4}$$

where $\mu_F(x)$ is the degree of membership x (between 0 and 1).

In the MPPT technique, FLC is used to find MPP with input in the form of error (E) and change of error (ΔE), while the output is in the form of PWM feed to control the converter duty cycle. The two inputs are obtained as

$$Error, E(k) = \frac{\Delta P}{\Delta V} = \frac{P(k) - P(k-1)}{V(k) - V(k-1)} \tag{5}$$

$$Change\ Error, \Delta E(k) = E(k) - E(k-1) \tag{6}$$

where (k) is the sample time, $P(k)$ is the power, $V(k)$ is the PV voltage. $P(k-1)$ and $V(k-1)$ are the previous PV power and voltage, respectively. $E(k)$ indicates the operating load point that is located to the left or right, while $\Delta E(k)$ in the direction of motion of the point.

In the FLC system design, there are three main components, namely fuzzification, inference, and defuzzification. In this work, the fuzzy Mamdani (min-max) model is employed.

A. FUZZIFICATION AND MEMBERSHIP FUNCTION

Fuzzification input in the form of crisp is then converted into fuzzy numbers into linguistic values. The inputs are then grouped into a membership function. Types of membership

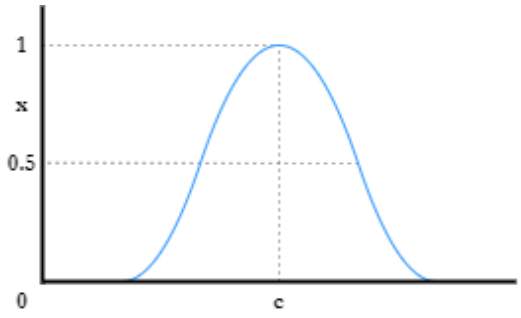

FIGURE 4. Gaussian membership function.

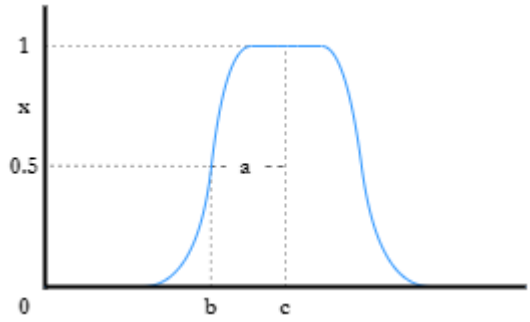

FIGURE 5. GBell membership function.

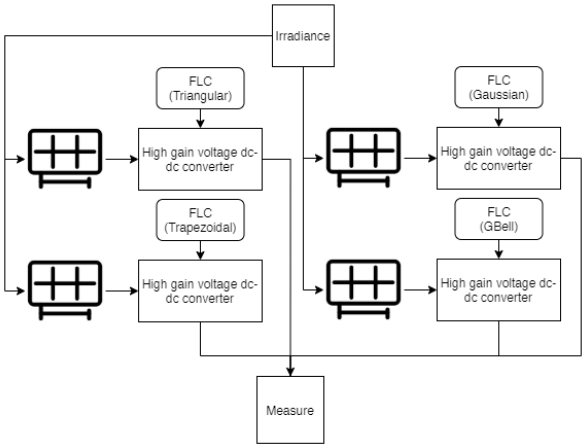

FIGURE 6. Block diagram of the system.

functions to be observed in this work are Triangular, Trapezoidal, Gaussian, and Generalized Bell (GBell). In this paper, the membership function is built with a symmetrical focused with 50% overlaps. Figure 2 to Figure 5 show the forms of the Triangular, Trapezoidal, Gaussian, and GBell membership function used, respectively. The mathematical equations for them are displayed sequentially in (7), (9), (11), and (12), respectively.

A Triangular curve as shown in Figure 2 is a combination of two linear lines, and it is determined by three parameters (a, b, c). The x coordinates of the three angles of the Triangular membership function are determined by parameters

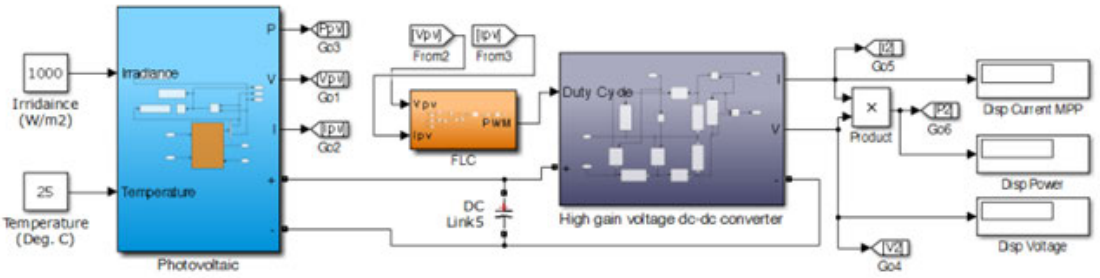

FIGURE 7. The developed system.

(a, b, c) with a < b < c. The Triangular curve is based on (7).

$$\text{triangle}\,(x; a, b, c) = \begin{cases} 0 & \text{for } x \le a \\ \dfrac{x-a}{b-a} & \text{for } a \le x \le b \\ \dfrac{c-x}{c-b} & \text{for } b \le x \le c \\ 0 & \text{for } x \ge c \end{cases} \tag{7}$$

where the parameters a, b, and c give the location of fuzzy membership function.

Using the min-max, (7) can be reformulated as (8).

$$\text{triangle}\,(x; a, b, c) = \max\left(\min\left(\frac{x-a}{b-a}, \frac{c-x}{c-b}, 0\right)\right) \tag{8}$$

Trapezoidal curve as shown in Figure 3 has a shape resembling a Triangular curve, but there is a membership value of 1 at several points. The difference from Triangular is that the Trapezoidal membership function has a flat top so it is not fuzzy. Trapezoidal membership function is built with four parameters (a, b, c, d). Then the Trapezoidal membership function is (9).

$$\text{trap}\,(x; a, b, c, d) = \begin{cases} 0 & \text{for } x \le a \\ \dfrac{x-a}{b-a} & \text{for } a \le x \le b \\ 1 & \text{for } b \le x \le c \\ \dfrac{d-x}{d-c} & \text{for } c \le x \le d \\ 0 & \text{for } x \ge d \end{cases} \tag{9}$$

where the parameters a, b, c and d give the location of fuzzy membership function.

Similar to Triangular, Trapezoidal membership function in (9) can be reformulated with the min-max as (10).

$$\text{trap}\,(x; a, b, c, d) = \max\left(\min\left(\frac{x-a}{b-a}, 1\frac{d-x}{d-c}, 0\right)\right) \tag{10}$$

Unlike Triangular membership function which has sharp peak, Gaussian as shown in Figure 4 has soft peak. Then the Gaussian membership function is (11).

$$\text{gauss}\,(x; \sigma, c) = e^{\frac{-(x-c)^2}{2\sigma^2}} \tag{11}$$

where x is the crisp variable.

TABLE 1. Fuzzy rule base.

		E				
		NB	NS	Z	PS	PB
ΔE	NB	NB	NB	Z	PB	PB
	NS	NS	NS	Z	PS	PS
	Z	Z	Z	Z	Z	Z
	PS	PS	PS	Z	NS	NS
	PB	PB	PB	Z	NB	NB

GBell membership function as shown in Figure 5 is generalized Cauchy distribution used in probability theory. Then the GBell membership function is (12).

$$\text{bell}\,(x; a, b, c) = \frac{1}{1 + \left|\frac{x-c}{a}\right|^{2m}} \tag{12}$$

where m defines the width of the flat top of the bell function.

B. INFERENCE

In this process, the grouped fuzzy input is calculated into the rule-base to determine the output. This rule-base serves to define the desired relationship rules between input and output variables. The number of rules depends on the number of input membership functions used. In this study, each input has five membership functions, 25 rules are obtained accordingly as shown in Table 1.

C. DEFUZZIFICATION

In the defuzzification process, fuzzy numbers are converted into crisp as the final output of the FLC. The defuzzification process is based on the center of gravity obtained by (13). The FLC output obtained is used to control the duty cycle (D) of the high gain voltage DC-DC converter.

$$D = \frac{\sum x_i \times \mu_i}{\sum \mu_i} \tag{13}$$

where D and x are the duty cycle and the output triangle value, respectively.

V. EXPERIMENTAL SETUP

In this work, the FLC algorithm is utilized on the MPPT technique for PV systems feed to a high gain voltage

TABLE 2. Parameters of the Trina Solar TSM-250PA05.08.

PV Parameters	Value
Module data	
Maximum Power (W)	249.86
Cells per module (N_{cell})	60
Open circuit voltage V_{oc} (V)	37.6
Short-circuit current I_{sc} (A)	8.55
Voltage at maximum power point V_{mp} (V)	31
Current at maximum power point I_{mp} (A)	8.06
Temperature coefficient of V_{oc} (%/°C)	-0.35
Temperature coefficient of I_{sc} (%/°C)	0.06
Module parameters	
Light-generated current IL (A)	8.5795
Diode saturation current ID (A)	2.0381e-10
Diode ideality factor	0.99766
Shunt resistance R_{sh} (Ω)	301.8149
Series resistance R_s (Ω)	0.247

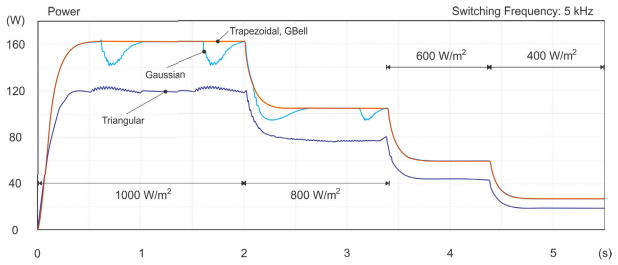

FIGURE 8. P_{out} with a switching frequency of 5 kHz.

DC-DC converter. The block diagram of the system is shown in Figure 6. Figure 7 shows a system consisting of a PV module, high gain voltage DC-DC converter with an MPPT controller connected to a load that has been created using MATLAB/Simulink. The PV model used is Trina Solar TSM-250PA05.08 with the specifications shown in Table 2.

VI. RESULTS AND DISCUSSION

In this work, the FLC algorithm has been successfully built on the MPPT technique for PV systems feed to a high gain voltage DC-DC converter. The resulting slope of each system created is then observed, and several vital parameters are recorded. The parameters measured are V_{out}, I_{out}, P_{out}, oscillation and tracking speed.

The testing is done by comparing the performance of membership functions including Triangular, Trapezoidal, Gaussian, and GBell. The switching frequency of the converter is varied for each membership function. The switching frequencies used are 5 kHz, 10 kHz, and 20 kHz. Furthermore, the irradiation variable is also varied at each switching frequency. The irradiation variations are 1000 W/m^2, 800 W/m^2, 600 W/m^2, and 400 W/m^2.

Tables 3 to 7 are the values for P_{out}, V_{out}, I_{out}, an oscillation and a tracking speed of the test results obtained, respectively. In Tables 3, 4, 5 and 6, the color-blocked values show the difference in values between Trapezoidal and GBell. The color green represents a better value than blue.

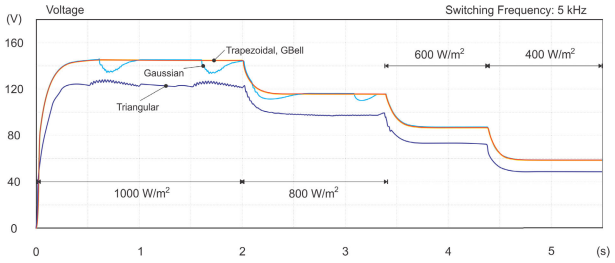

FIGURE 9. V_{out} with a switching frequency of 5 kHz.

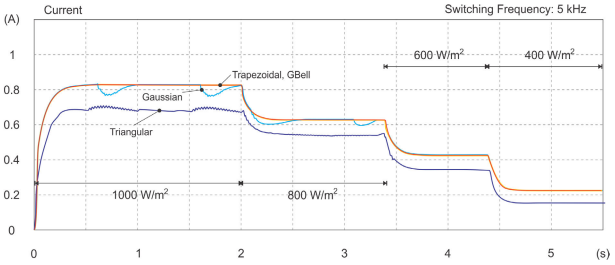

FIGURE 10. I_{out} with a switching frequency of 5 kHz.

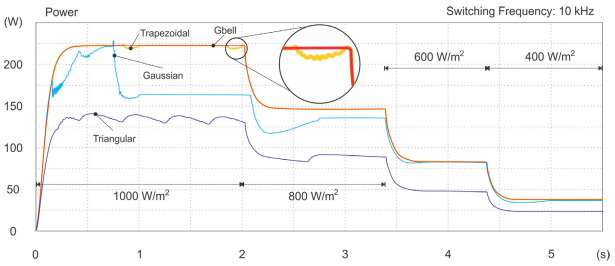

FIGURE 11. P_{out} with a switching frequency of 10 kHz.

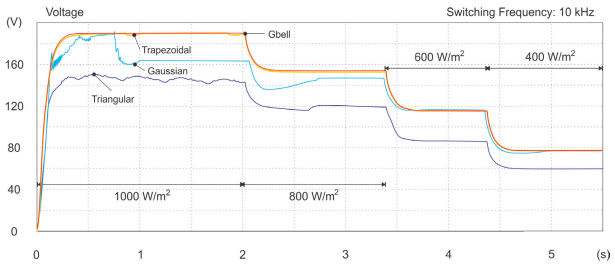

FIGURE 12. V_{out} with a switching frequency of 10 kHz.

Figures 8 to 10 show the P_{out}, V_{out}, and I_{out} slope of the four membership functions that were tested with a switching frequency of 5 kHz, respectively. It appears that Trapezoidal, Gaussian, and GBell produce a larger output than the Triangular. Furthermore, the tracking speed of the three membership functions is faster in reaching MPP. This is shown in Table 7 where Trapezoidal, Gaussian, and GBell have the same tracking speed. However, shown in Table 6, Gaussian has more significant oscillations than the other three memberships. In this test, the Trapezoidal and GBell produce similar output, oscillations, and tracking speeds.

TABLE 3. P_{out} at the switching frequency and irradiance are varied.

	Switching Frequency											
	5 kHz				10 kHz				20 kHz			
	Irradiance											
	1000	800	600	400	1000	800	600	400	1000	800	600	400
Membership Function	Watt (W)											
Triangular	122.52	76.55	44.25	19.02	130.50	88.010	46.43	22.74	155.30	115.80	60.86	25.44
Trapezoidal	162.75	104.52	58.98	26.27	221.60	145.20	82.05	36.62	229.50	166.00	105.70	54.90
Gaussian	162.75	104.52	58,98	26.27	171.70	135.10	82.05	36.41	219.30	129.30	68.80	33.57
GBell	162.75	104.52	58.98	26.27	221.60	82 .20	82.05	36.62	229.80	172.90	106.20	51.76

TABLE 4. V_{out} at the switching frequency and irradiance are varied.

	Switching Frequency											
	5 kHz				10 kHz				20 kHz			
	Irradiance											
	1000	800	600	400	1000	800	600	400	1000	800	600	400
Membership Function	Volt (V)											
Triangular	138.55	110.85	84.15	56.50	144.50	118.70	86.19	60.32	157.20	136.10	98.68	63.80
Trapezoidal	161.55	129.33	97.16	64.83	188.30	152.40	114.60	76.55	191.60	163.00	130.10	93.12
Gaussian	161.55	129.33	97.16	64.83	187.90	147.00	114.60	76.32	187.30	143.90	104.90	73.28
GBell	161.55	129.33	97.16	64.83	188.30	152.40	114.60	76.55	191.80	166.30	130.40	91.00

TABLE 5. I_{out} at the switching frequency and irradiance are varied.

	Switching Frequency											
	5 kHz				10 kHz				20 kHz			
	Irradiance											
	1000	800	600	400	1000	800	600	400	1000	800	600	400
Membership Function	Ampere (I)											
Triangular	0.8843	0.6906	0.5258	0.3532	0.9030	0.7417	0.5387	0.3770	0.9853	0.8506	0.6108	0.3987
Trapezoidal	1.0086	0.8082	0.6070	0.4052	1.1770	0.9527	0.7161	0.4784	1.1980	1.0190	0.8130	0.5820
Gaussian	1.0086	0.8082	0.6070	0.4052	1.1750	0.9189	0.7161	0.4770	1.1710	0.8991	0.6557	0.4580
GBell	1.0086	0.8082	0.6070	0.4052	1.1770	0.9527	0.7161	0.4784	1.1980	1.0400	0.8149	0.5688

TABLE 6. Oscillation at the switching frequency and irradiance are varied.

	Switching Frequency											
	5 kHz				10 kHz				20 kHz			
	Irradiance											
	1000	800	600	400	1000	800	600	400	1000	800	600	400
Membership Function	Volt (V)											
Triangular	1.816	1.550	0.384	0.321	7.279	3.815	0.258	0.164	12.680	1.036	0.657	0.314
Trapezoidal	0.184	0.171	0.169	0.166	1.625	0.076	0.016	0.013	0.653	0.392	0.378	0.364
Gaussian	13.820	12.460	0.169	0.166	12.500	8.952	0.116	0.113	11.990	8.348	0.291	0.089
GBell	0.184	0.171	0.169	0.166	0.049	0.046	0.016	0.013	0.392	0.231	0.188	0.077

TABLE 7. Tracking speed at the switching frequency and irradiance are varied.

	Switching Frequency											
	5 kHz				10 kHz				20 kHz			
	Irradiance											
	1000	800	600	400	1000	800	600	400	1000	800	600	400
Membership Function	Second (s)											
Triangular	0.40	0.40	0.27	0.22	0.40	0.39	0.28	0.25	0.40	0.25	0.18	0.15
Trapezoidal	0.35	0.35	0.27	0.22	0.35	0.35	0.28	0.25	0.27	0.25	0.18	0.15
Gaussian	0.35	0.35	0.27	0.22	0.35	0.35	0.28	0.25	0.27	0.25	0.18	0.15
GBell	0.35	0.35	0.27	0.22	0.35	0.35	0.28	0.25	0.27	0.25	0.18	0.15

TABLE 8. Comparison between trapezoidal and GBell at switching frequency 20 kHz.

	Switching Frequency 20 kHz											
	P_{out}			V_{out}			I_{out}			Oscillation		
	1000	800	600	1000	800	600	1000	800	600	1000	800	600
Membership Function	Watt (W)			Volt (V)			Ampere (I)			Volt (V)		
Trapezoidal	229.50	166.00	105.70	191.60	163.00	130.10	1.1980	1.0190	0.8130	0.653	0.392	0.378
GBell	229.80	172.90	106.20	191.80	166.30	130.40	1.1980	1.0400	0.8149	0.392	0.231	0.188

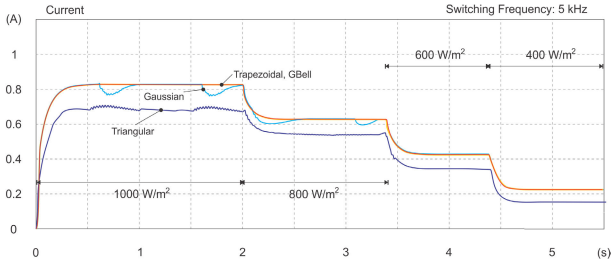

FIGURE 13. I_{out} with a switching frequency of 10 kHz.

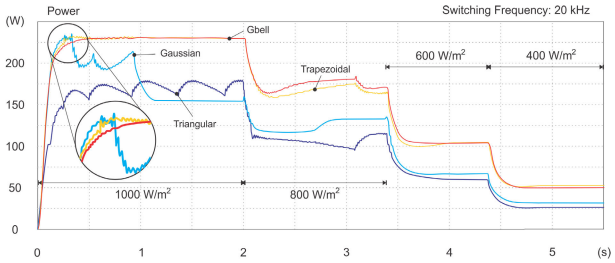

FIGURE 14. P_{out} with a switching frequency of 20 kHz.

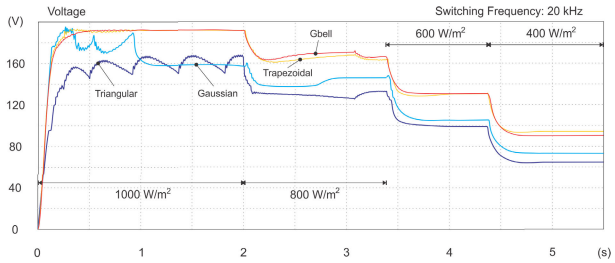

FIGURE 15. V_{out} with a switching frequency of 20 kHz.

Trapezoidal and GBell performance is slightly different in tests with a switching frequency of 10 kHz. Figures 11 to 13 show the slope P_{out}, V_{out}, and I_{out} for testing with a switching frequency of 10 kHz, respectively. It is shown from the result obtained in Table 6, the Trapezoidal experiences periodic oscillations of 1.625% at 1000 W/m^2 irradiation at a steady-state condition. However, the output value, oscillation, and tracking speed are still superior to Gaussian and Triangular.

In the test with a switching frequency of 20 kHz, the performance of Trapezoidal and GBell are decreased. The oscillations of these two membership levels increase overall, at high and low irradiation. At low irradiation levels, V_{out}, hence P_{out}, are generated with a lower GBell than Trapezoidal. However, the resulting oscillations are still within an acceptable range.

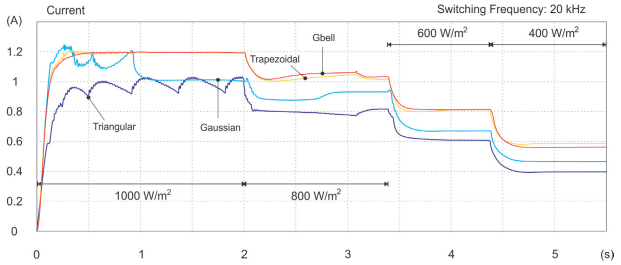

FIGURE 16. I_{out} with a switching frequency of 20 kHz.

The V_{out} and P_{out} produced by GBell are higher than Trapezoidal. The output of P_{out}, V_{out}, and I_{out} with a switching frequency of 20 kHz are shown in Figures 14 to 16.

Based on the tests carried out by varying the irradiation and switching frequency, it is seen that GBell outperforms other fuzzy membership function types in terms of converter output optimization, oscillation, and tracking speed.

A head-to-head comparison of performance between Trapezoidal and GBell is shown in Table 8. The variables compared are P_{out}, V_{out}, I_{out}, and oscillation at 20 kHz switching frequency and irradiation variation between 1000 W/m^2 to 600W/m^2. Based on the result, GBell outperforms the Trapezoidal in terms of performance.

The shape of the fuzzy membership function has an impact on the optimization results. However, the best shape of fuzzy membership function in one case may not necessarily show similar performance in other cases. Previous research evaluated fuzzy MF to control induction motor drive by Zhao and Bose [47]. The evaluation results show that Triangular provides superior performance than other membership function forms (Trapezoidal, Gaussian, Bell-shaped, Sigmoid, and Polynomial) in terms of reducing overshoot, undershoot, speed in response, recovery, and steady-state accuracy. The evaluation also shows that the Trapezoidal performance is close to the Triangular. The contrast result is shown in this study, where fuzzy membership function is evaluated for MPP tracking using a high gain voltage DC-DC converter. The GBell shape provides the most superior performance among other membership functions. Trapezoidal arrives as the second alternative.

VII. CONCLUSION

This paper discussed the different membership function effects, namely Triangular, Trapezoidal, Gaussian, and GBell which are utilized to construct fuzzy logic controller (FLC) for maximum power point tracking (MPPT) of solar photovoltaic (PV). The proposed high gain voltage

DC-DC converter is employed to the building system. Several parameters were observed by changing the switching frequency and irradiation variables. The results obtained indicate that the application of GBell and Trapezoidal outperform Triangular and Gaussian membership functions. Furthermore, these two membership function types (*i.e.* GBell and Trapezoidal) have comparable results during operation at 5 kHz or 10 kHz switching frequencies. In addition, GBell shows superior performance over Trapezoidal when the switching frequency is increased to 20 kHz.

REFERENCES

[1] S. Messalti, A. Harrag, and A. Loukriz, "A new variable step size neural networks MPPT controller: Review, simulation and hardware implementation," *Renew. Sustain. Energy Rev.*, vol. 68, pp. 221–233, Feb. 2017.

[2] A. K. Podder, N. K. Roy, and H. R. Pota, "MPPT methods for solar PV systems: A critical review based on tracking nature," *IET Renew. Power Gener.*, vol. 13, no. 10, pp. 1615–1632, Jul. 2019.

[3] T. Abderrahim, T. Abdelwahed, and M. Radouane, "Improved strategy of an MPPT based on the sliding mode control for a PV system," *Int. J. Electr. Comput. Eng.*, vol. 10, no. 3, p. 3074, Jun. 2020.

[4] K. Sundareswaran, S. Peddapati, and S. Palani, "Application of random search method for maximum power point tracking in partially shaded photovoltaic systems," *IET Renew. Power Gener.*, vol. 8, no. 6, pp. 670–678, 2014.

[5] N. Bizon, "Global maximum power point tracking (GMPPT) of photovoltaic array using the extremum seeking control (ESC): A review and a new GMPPT ESC scheme," *Renew. Sustain. Energy Rev.*, vol. 57, pp. 524–539, May 2016.

[6] A. Kheldoun, R. Bradai, R. Boukenoui, and A. Mellit, "A new golden section method-based maximum power point tracking algorithm for photovoltaic systems," *Energy Convers. Manage.*, vol. 111, pp. 125–136, Mar. 2016.

[7] E. Koutroulis, K. Kalaitzakis, and N. C. Voulgaris, "Development of a microcontroller-based, photovoltaic maximum power point tracking control system," *IEEE Trans. Power Electron.*, vol. 16, no. 1, pp. 46–54, Jan. 2001.

[8] J. Appelbaum, "The operation of loads powered by separate sources or by a common source of solar cells," *IEEE Trans. Energy Convers.*, vol. 4, no. 3, pp. 351–357, Sep. 1989.

[9] J. H. R. Enslin and D. B. Snyman, "Combined low-cost, high-efficient inverter, peak power tracker and regulator for PV applications," *IEEE Trans. Power Electron.*, vol. 6, no. 1, pp. 73–82, Jan. 1991.

[10] J. H. R. Enslin, M. S. Wolf, D. B. Snyman, and W. Swiegers, "Integrated photovoltaic maximum power point tracking converter," *IEEE Trans. Ind. Electron.*, vol. 44, no. 6, pp. 769–773, Dec. 1997.

[11] S. J. Chiang, K. T. Chang, and C. Y. Yen, "Residential photovoltaic energy storage system," *IEEE Trans. Ind. Electron.*, vol. 45, no. 3, pp. 385–394, Jun. 1998.

[12] T.-F. Wu, C.-H. Chang, and Y.-J. Wu, "Single-stage converters for PV lighting systems with MPPT and energy backup," *IEEE Trans. Aerosp. Electron. Syst.*, vol. 35, no. 4, pp. 1306–1317, Oct. 1999.

[13] N. Kasa, T. Lida, and H. Iwamoto, "Maximum power point tracking with capacitor identifier for photovoltaic power system," *IEE Proc., Electr. Power Appl.*, vol. 147, no. 6, pp. 497–502, Nov. 2000.

[14] F. Giraud and Z. M. Salameh, "Analysis of the effects of a passing cloud on a grid-interactive photovoltaic system with battery storage using neural networks," *IEEE Trans. Energy Convers.*, vol. 14, no. 4, pp. 1572–1577, Dec. 1999.

[15] Y.-C. Kuo, T.-J. Liang, and J.-F. Chen, "Novel maximum-power-point-tracking controller for photovoltaic energy conversion system," *IEEE Trans. Ind. Electron.*, vol. 48, no. 3, pp. 594–601, Jun. 2001.

[16] M. Seyedmahmoudian, B. Horan, T. K. Soon, R. Rahmani, A. M. Than, S. Mekhilef, and A. Stojcevski, "State of the art artificial intelligence-based MPPT techniques for mitigating partial shading effects on PV systems—A review," *Renew. Sustain. Energy Rev.*, vol. 64, pp. 435–455, Oct. 2016.

[17] A. Mohapatra, B. Nayak, P. Das, and K. B. Mohanty, "A review on MPPT techniques of PV system under partial shading condition," *Renew. Sustain. Energy Rev.*, vol. 80, pp. 854–867, Dec. 2017.

[18] A. Jusoh, R. Alik, T. K. Guan, and T. Sutikno, "MPPT for PV system based on variable step size P&O algorithm," *Telkomnika*, vol. 15, no. 1, p. 79, 2017.

[19] A. Jusoh, T. Sutikno, T. K. Guan, and S. Mekhilef, "A review on favourable maximum power point tracking systems in solar energy application," *Telkomnika*, vol. 12, no. 1, p. 6, Mar. 2014.

[20] B. Yang, T. Zhu, J. Wang, H. Shu, T. Yu, X. Zhang, W. Yao, and L. Sun, "Comprehensive overview of maximum power point tracking algorithms of PV systems under partial shading condition," *J. Cleaner Prod.*, vol. 268, Sep. 2020, Art. no. 121983.

[21] B. Subudhi and R. Pradhan, "A comparative study on maximum power point tracking techniques for photovoltaic power systems," *IEEE Trans. Sustain. Energy*, vol. 4, no. 1, pp. 89–98, Jan. 2013.

[22] C. R. Algarín, J. T. Giraldo, and O. R. Álvarez, "Fuzzy logic based MPPT controller for a PV system," *Energies*, vol. 10, no. 12, p. 2036, Dec. 2017.

[23] A. Youssef, M. E. Telbany, and A. Zekry, "Reconfigurable generic FPGA implementation of fuzzy logic controller for MPPT of PV systems," *Renew. Sustain. Energy Rev.*, vol. 82, pp. 1313–1319, Feb. 2018.

[24] H. Rezk, M. Aly, M. Al-Dhaifallah, and M. Shoyama, "Design and hardware implementation of new adaptive fuzzy logic-based MPPT control method for photovoltaic applications," *IEEE Access*, vol. 7, pp. 106427–106438, 2019.

[25] B. N. Alajmi, K. H. Ahmed, S. J. Finney, and B. W. Williams, "A maximum power point tracking technique for partially shaded photovoltaic systems in microgrids," *IEEE Trans. Ind. Electron.*, vol. 60, no. 4, pp. 1596–1606, Apr. 2013.

[26] M. Rakhshan, N. Vafamand, M.-H. Khooban, and F. Blaabjerg, "Maximum power point tracking control of photovoltaic systems: A polynomial fuzzy model-based approach," *IEEE J. Emerg. Sel. Topics Power Electron.*, vol. 6, no. 1, pp. 292–299, Mar. 2018.

[27] A. El Khateb, N. A. Rahim, J. Selvaraj, and M. N. Uddin, "Fuzzy-logic-controller-based SEPIC converter for maximum power point tracking," *IEEE Trans. Ind. Appl.*, vol. 50, no. 4, pp. 2349–2358, Jul./Aug. 2014.

[28] S. Tang, Y. Sun, Y. Chen, Y. Zhao, Y. Yang, and W. Szeto, "An enhanced MPPT method combining fractional-order and fuzzy logic control," *IEEE J. Photovolt.*, vol. 7, no. 2, pp. 640–650, Mar. 2017.

[29] U. Yilmaz, A. Kircay, and S. Borekci, "PV system fuzzy logic MPPT method and PI control as a charge controller," *Renew. Sustain. Energy Rev.*, vol. 81, pp. 994–1001, Jan. 2018.

[30] Z. Sun and Z. Yang, "Improved maximum power point tracking algorithm with cuk converter for PV systems," *J. Eng.*, vol. 2017, no. 13, pp. 1676–1681, Jan. 2017.

[31] B. Bendiba, F. Krim, H. Belmili, M. F. Almi, and S. Boulouma, "Advanced fuzzy MPPT controller for a stand-alone PV system," *Energy Proc.*, vol. 50, pp. 383–392, Jun. 2014.

[32] H. Rezk and A. M. Eltamaly, "A comprehensive comparison of different MPPT techniques for photovoltaic systems," *Solar Energy*, vol. 112, pp. 1–11, Feb. 2015.

[33] R. Boukenoui, H. Salhi, R. Bradai, and A. Mellit, "A new intelligent MPPT method for stand-alone photovoltaic systems operating under fast transient variations of shading patterns," *Sol. Energy*, vol. 124, pp. 124–142, Feb. 2016.

[34] Y.-T. Chen, Y.-C. Jhang, and R.-H. Liang, "A fuzzy-logic based auto-scaling variable step-size MPPT method for PV systems," *Sol. Energy*, vol. 126, pp. 53–63, Mar. 2016.

[35] A. H. E. Khateb, N. A. Rahim, and J. Selvaraj, "Fuzzy logic control approach of a maximum power point employing SEPIC converter for standalone photovoltaic system," *Proc. Environ. Sci.*, vol. 17, pp. 529–536, 2013.

[36] M. Kermadi and E. M. Berkouk, "Artificial intelligence-based maximum power point tracking controllers for photovoltaic systems: Comparative study," *Renew. Sustain. Energy Rev.*, vol. 69, pp. 369–386, Mar. 2017.

[37] M. B. Kalashani and M. Farsadi, "New structure for photovoltaic systems with maximum power point tracking ability," *Int. J. Power Electron. Drive Syst.*, vol. 4, no. 4, p. 489, Dec. 2014.

[38] T. H. Kwan and X. Wu, "Maximum power point tracking using a variable antecedent fuzzy logic controller," *Sol. Energy*, vol. 137, pp. 189–200, Nov. 2016.

[39] S. Hajighorbani, M. A. M. Radzi, M. Z. A. A. Kadir, S. Shafie, R. Khanaki, and M. R. Maghami, "Evaluation of fuzzy logic subsets effects on maximum power point tracking for photovoltaic system," *Int. J. Photoenergy*, vol. 2014, Sep. 2014, Art. no. 719126.

[40] O. A. M. Ali, A. Y. Ali, and B. S. Sumait, "Comparison between the effects of different types of membership functions on fuzzy logic controller performance," *Int. J.*, vol. 76, pp. 76–83, Mar. 2015.
[41] C.-S. Chiu, "T-S fuzzy maximum power point tracking control of solar power generation systems," *IEEE Trans. Energy Convers.*, vol. 25, no. 4, pp. 1123–1132, Dec. 2010.
[42] J. P. Ram, T. S. Babu, and N. Rajasekar, "A comprehensive review on solar PV maximum power point tracking techniques," *Renew. Sustain. Energy Rev.*, vol. 67, pp. 826–847, Jan. 2017.
[43] E. Kandemir, N. S. Cetin, and S. Borekci, "A comprehensive overview of maximum power extraction methods for PV systems," *Renew. Sustain. Energy Rev.*, vol. 78, pp. 93–112, Oct. 2017.
[44] W. I. Hameed, A. L. Saleh, B. A. Sawadi, Y. I. A. Al-Yasir, and R. A. Abd-Alhameed, "Maximum power point tracking for photovoltaic system by using fuzzy neural network," *Inventions*, vol. 4, no. 3, p. 33, Jun. 2019.
[45] S. H. Hanzaei, S. A. Gorji, and M. Ektesabi, "A scheme-based review of MPPT techniques with respect to input variables including solar irradiance and PV arrays' temperature," *IEEE Access*, vol. 8, pp. 182229–182239, 2020.
[46] P. A. Dahono, "New step-up DC-DC converters for PV power generation systems," in *Proc. Int. Seminar Intell. Technol. Appl. (ISITIA)*, Aug. 2017, pp. 187–192.
[47] J. Zhao and B. K. Bose, "Evaluation of membership functions for fuzzy logic controlled induction motor drive," in *Proc. IEEE 28th Annu. Conf. Ind. Electron. Soc. (IECON)*, vol. 1. IEEE, 2002, pp. 229–234, doi: 10.1109/IECON.2002.1187512.

TOLE SUTIKNO (Member, IEEE) received the B.E. degree from Universitas Diponegoro, in 1999, the M.E. degree from Universitas Gadjah Mada, in 2004, and the Ph.D. degree from Universiti Teknologi Malaysia, in 2016, all in electrical engineering. He has been an Associate Professor with Universitas Ahmad Dahlan (UAD), Yogyakarta, Indonesia, since 2008. He is currently a Lecturer with the Electrical Engineering Department, UAD. He has been the Editor-in-Chief of the *TELKOMNIKA*, since 2005, and the Leader of the Embedded Systems and Power Electronics Research Group, since 2016. His current research interests include digital design, industrial applications, industrial electronics, industrial informatics, power electronics, motor drives, renewable energy, FPGA applications, embedded systems, artificial intelligence, intelligent control, and information and digital technologies.

ARSYAD CAHYA SUBRATA received the B.E. degree in electrical engineering from Universitas Ahmad Dahlan, Indonesia, in 2016, and the M.E. degree in electrical engineering from Universitas Diponegoro, Indonesia, in 2020. He is currently a Research Assistant at the Embedded Systems and Power Electronics Research Group (ESPERG), since 2018. His current research interests include artificial intelligent, digital control systems, renewable energy, and intelligent control systems.

AHMAD ELKHATEB (Senior Member, IEEE) is currently a Lecturer of power electronics with the School of Electronics, Electrical Engineering and Computer Science, Queen's University, Belfast, U.K. His current research interests include power electronics, DC/DC converters, power generation, and grid integration. He is a fellow of Higher Education Academy, U.K.; a member of the ESPSRC Associate Review College; and an Associate Editor of IEEE Access and the *IET Power Electronics*.